Published in final edited form as:
Circ Res. 2010 August 20; 107(4): 558–568. doi:10.1161/CIRCRESAHA.110.224634.

Genetic Architecture Underlying Variation in Extent and Remodeling of the Collateral Circulation

Shiliang Wang, BS[*], **Hua Zhang, MD**[*], **Xuming Dai, MD PhD**, **Robert Sealock, PhD**, and **James E. Faber, PhD**
Department of Cell and Molecular Physiology and the McAllister Heart Institute, University of North Carolina at Chapel Hill

Abstract

Rationale—Collaterals are arteriole-to-arteriole anastomoses that connect adjacent arterial trees. They lessen ischemic tissue injury by serving as endogenous bypass vessels when the trunk of one tree becomes narrowed by vascular disease. The number and diameter ("extent") of native (pre-existing) collaterals, plus their amount of lumen enlargement (growth/remodeling) in occlusive disease, show remarkably wide variation among inbred mouse strains (eg, C57BL/6 and BALB/c), resulting in large differences in tissue injury in models of occlusive disease. Evidence suggests similar large differences exist among healthy humans.

Objective—To identify candidate loci responsible for genetic-dependent collateral variation.

Methods and Results—Cerebral collateral number and diameter were determined in 221 C57BL/6-x-BALB/c F2 progeny, followed by linkage analysis to identify quantitative trait loci (QTL) for collateral number and diameter. Four QTL were obtained for collateral number, including epistasis between two loci. A QTL that was identical to the strongest QTL for collateral number on chromosome 7 (LOD=29, effect size=37%) was also mapped for collateral diameter (LOD=17, effect size=30%). Chromosome substitution strain analysis confirmed this locus. We also obtained a unique QTL on chromosome 11 for collateral remodeling after middle cerebral artery occlusion. Association mapping within the chromosome 7 QTL interval using collateral traits measured for 15 inbred strains, delineated 172k (p=0.00002) and 290k (p=0.0004) base-pair regions on chromosome 7 containing 2 and 9 candidate genes, respectively.

Conclusions—We conclude that collateral extent and remodeling are unique, highly heritable complex traits, with one QTL predominantly affecting native collateral number and diameter.

Keywords

Collateral vessels; genetics; quantitative trait loci; cerebral circulation; arteriogenesis

Atherosclerotic, atherothrombotic and thromboembolic occlusive vascular diseases constitute the primary cause of morbidity and mortality in developed countries. Many physiological systems are concomitantly recruited, albeit with significant inter-individual

Corresponding author: James E. Faber, PhD., Department of Cell and Molecular Physiology, 6309 MBRB, University of North Carolina, Chapel Hill, NC 27599-7545. Tel: 919-966-0327. Fax: 919-966-6927. jefaber@med.unc.edu.
[*]Equal contribution.

Disclosures
None

variation, which lessen the accompanying ischemic tissue injury. Among these, three vascular protective mechanisms are paramount: (1) the number and diameter of arteriole-to-arteriole anastomoses present in the tissue before the onset of disease that cross-connect occasional distal-most arterioles of adjacent trees (ie, the “native collateral extent”), (2) an anatomic increase in lumen diameter and wall thickness of these vessels caused by obstruction of flow to one of the trees—a process termed collateral remodeling, collateral growth or arteriogenesis, and (3) ischemic angiogenesis, ie, the sprouting of additional capillaries (1–6). Arteriogenesis, which requires days-to-weeks to achieve up to an approximately 10-fold increase in diameter depending on tissue and species, occurs when perfusion of an adjacent tree is chronically reduced below a critical level. This increases flow-dependent shear stress on collateral endothelial cells, which in turn initiates an inflammatory-like remodeling process. It is becoming recognized that the extent of the native collateral circulation and collateral remodeling have significantly greater impact on restoring blood flow to ischemic tissue than does angiogenesis—which can only increase dispersion of whatever flow is provided by the collateral network (1,5,6).

The severity of the clinical manifestations of occlusive vascular diseases, ie, myocardial infarction, stroke and chronic ischemic disease of the heart, brain and lower extremities, have long been known to vary widely among individuals. This is presumably due to variation in environmental influences and risk factors as well as genetic mutations and polymorphisms affecting the extant pathological and physiological processes. Although much effort has focused on identifying the sources of this variation, the possibility that differences in extent of the native collateral circulation exist among healthy individuals and contribute significantly when disease strikes has, until recently, received little attention. Meier and colleagues (7) found, using an index primarily dependent on collateral density and diameter, that coronary collateral conductance varied by approximately 10-fold in healthy human subjects. Since these subjects lacked coronary artery disease, the variation could not be affected by differences in stenosis-induced collateral remodeling. Studies employing dynamic angiography in patients with acute stroke from middle cerebral artery obstruction, where differences in remodeling can again be ruled out due to the acute nature, suggest that wide variation in native collateral conductance is also present in the cerebral circulation (8–11). Likewise, evidence exists for significant variation in collateral extent in the peripheral limbs of healthy individuals (12,13).

Recent studies in mice suggest that a substantial amount of this variability arises from naturally occurring polymorphisms in genetic loci involved in molecular pathways directing formation of the collateral circulation, which occurs late embryonically and early postnatally in mice (14). Native collateral density and diameter evidenced large differences in multiple tissues in adult C57BL/6 and BALB/c mouse strains (15–17). In fact, C57BL/6 and BALB/c mice have the largest extremes in collateral extent in the cerebral circulation among 15 strains, for example exhibiting a greater than 30-fold difference in collateral density (16). Importantly, these differences in collateral extent in the cerebral circulation are shared qualitatively by other tissues, including skeletal muscle and intestine (16,19,20). Moreover, the rank-order of cerebral collateral extent among 15 mouse strains closely predicts the rank-order of severity of stroke (infarct volume) after permanent middle cerebral artery occlusion (18). This finding establishes a major role for genetic variation in the extent of the collateral circulation in determining variation in severity of ischemic tissue injury. Interestingly, collateral remodeling during stroke also evidenced significant variation, but with a strain-specific pattern significantly different from the pattern associating infarct volume with collateral extent (18). This suggests that different pathways are responsible for collateral formation versus collateral remodeling, and that genetic variation in them is likely to be mediated by different loci.

Nothing is known about the genetic loci responsible for the remarkably wide variation in native collateral extent and collateral remodeling described above. However, studies employing gene targeting methods have identified two genes, *Vegfa* and *Clic4*, whose expression positively regulates collateral formation in the embryo and thus collateral extent in the adult; one of these (*Vegfa*) also participates in collateral remodeling (19,20). Hence, polymorphisms in these genes are *a priori* candidates for causing variation in collateral circulatory function. Identification of the alleles underlying individual variation in collateral extent and remodeling is important not only to help define the responsible signaling pathways for these two processes, but also to allow assessment of risk-severity if occlusive vascular disease develops and to permit stratification of individuals enrolled in clinical trials testing new collaterogenic therapies. Therefore, in the present study we sought to identify genetic loci governing variation in collateral extent and remodeling. To achieve this goal we created 243 F2 mice intercrossed between the C57BL/6 and BALB/c strains and performed linkage analysis to identify quantitative trait loci (QTL). We then used association mapping among 15 inbred strains to identify candidate genes responsible for variation in collateral function.

Methods

Animals

F1 progeny obtained from reciprocal matings of C57BL/6J (B6) and BALB/cByJ (BALB/c, Bc) were mated to produce an F2 population. Chromosome substitution strains were C57BL/6J-Chr7A/J/NaJ (CSS7) and C57BL/6J-Chr17A/J/NaJ (CSS17).

Phenotyping

Mice were subjected to right-side middle cerebral artery occlusion (MCAO) and collateral number and diameter measured 6 days later (18). To image the pial circulation, the rostral vasculature was maximally dilated, filled with yellow Microfil™ with viscosity adjusted to prevent capillary filling, and fixed (paraformaldehyde). Collaterals connecting the anterior cerebral (ACA) and middle cerebral (MCA) artery trees in both hemispheres were digitally imaged. Cortical territories supplied by the MCA, ACA and PCA trees were determined (18). ANOVA or t-tests were used together with Bonferroni correction where appropriate.

DNA isolation and genotyping

Tail genomic DNA was genotyped using the 377-SNP GoldenGate genotyping array (Illumina, San Diego, CA). Manual genotyping was done for one marker (rs32420445). SNP positions were obtained from Build 37.1 of the NCBI SNP database.

Linkage analysis

Collateral traits are defined as collateral number, diameter and "conductance" (number-x-diameter) measured in the left (non-occluded) hemisphere. The remodeling trait is the average fold change in collateral diameter between right and left hemisphere 6 days after MCAO. These traits in the F2 population were subjected to linkage analysis using single and multiple QTL models in the R statistical program. Thresholds for significant and suggestive QTL were defined as P=0.05 and P=0.63, respectively.

Association mapping

The efficient mixed model association algorithm (EMMA; 21) was applied in R to collateral number measurements on 15 inbred strains, 8–10 individuals each, obtained previously (18) (see Online Figure I).

An expanded Materials and Methods section is available in the Online Data Supplement at http://circres.ahajournals.org.

Results

Native collateral trait differences between B6 and Bc strains are heritable

We previously showed in multiple tissues that Bc mice have smaller collateral number and diameters than B6 mice (16). This is striking in the pial circulation, where Bc mice average less than one collateral per hemisphere, compared to 9 in B6. We further showed that among 15 strains Bc had the lowest pial collateral number and near-lowest diameter (13μm) (18). Among those strains, B6 has the largest collateral diameter (23μm), and nearly the largest number of pial collaterals. Therefore, B6 and Bc were chosen for identification of QTL for native pial collateral number and diameter, for a quasi-index of total collateral "conductance" (defined as number-x-diameter) and for increase in collateral diameter (remodeling) induced by MCAO. MCAO in one hemisphere does not alter collateral number or diameter in the other, non-operated hemisphere (18). After exclusion of 22 individuals for poor filling or other technical problems, 221 F2 mice were analyzed for native collateral properties and 190 for remodeling. The mice were genotyped at 228 informative SNPs across the genome (see Methods).

Cerebral arteriograms from non-operated B6 and Bc mice are shown in Figure 1A. The entire population of MCA-ACA collaterals is confined to the pial surface, aiding direct quantification (18). The Bc brain shown, with no pial collaterals, is typical of most Bc mice. Previously reported values for collateral diameter and number in B6 and Bc (16,18) were confirmed here: 9 and 22.5um in B6, 0.5 and 12.5um in Bc) (Figure 1B).

All 3 collateral parameters were intermediate in the F1 population between those for B6 and Bc (Figure 1B) although closer to those for B6. Collateral diameter and conductance in F1 mice were significantly lower than in B6 ($p<0.05$) but were still larger than the average of B6 and Bc values. For collateral number, the trend toward fewer than in B6 was not significant. Thus, collateral traits in B6 are semi-dominant over Bc.

Genome-wide single QTL mapping detects a major effect on chromosome 7 (*Canq1*) for native collateral traits

In the F2 population, all 3 collateral traits were approximately normally distributed, indicative of polygenic traits, with the distributions containing suggestions that they may be sums of multiple normal distributions (Figure 1C). These traits were independent of sex, parental origin, or body weight (Online figures II, III). Variation in collateral traits was also independent of body weight among 15 inbred strains (18). Collateral number and diameter were minimally correlated ($r^2=0.13$), confirming previous results (18) and suggesting that number and diameter are largely independent traits (Online figure IV).

The phenotype-genotype data were subjected to genome-wide LOD score profiling using the single QTL model in R/QTL. This identified a single, highly significant locus on distal chromosome 7 for all 3 collateral traits (LOD scores of 21, 17, and 27 for number, diameter, and conductance, respectively; genetic (heritable) effect sizes≥30% for all three) (Figure 2A; Online table I). The peak is located 0.5cM telomeric to marker rs13479513 (134.25Mb; Figure 2A inset). The 95% confidence level is 62–67cM, which is estimated to correspond to 132.4–135.8Mb in physical location. The single QTL model also identified a significant QTL (genome-wide 0.05 significance level) for collateral number on chromosome 1, two suggestive QTL (genome-wide 0.63 significance level) on proximal chromosome 6 and chromosome 10 for number, and two suggestive QTL on chromosomes 1 and 10 for conductance (Figure 2A).

Additional QTL and epistasis identified by genome-wide multiple QTL mapping

Experiments using haplo-insufficient and null gene targeted mice have shown that *Vegfa*, *Flt1* (VEGFR1) and *Clic4* expression levels are strong positive determinants of collateral number (19; Lucitti and Faber, unpublished data; 20). However, our single QTL analysis revealed no QTL in the regions of these genes (Figure 2A), possibly due to the predominant major effect on chromosome 7. Moreover, the multiple suggestive QTL identified using the single QTL model suggest a complex genetic architecture may underlie variation in native collateral extent. Also, a single QTL model cannot detect epistasis. To address these issues, we subjected the data to genome-wide multiple QTL profiling with increased statistical power using the Stepwiseqtl function in R/QTL.

As shown in Figure 2B, this analysis confirmed and strengthened the QTL on chromosome 7 for collateral number, the LOD score improving from 21 to 29 and the effect size increasing from 32% to 37%. It also gave a strong QTL (LOD score 13) at 45cM (90Mb) on chromosome 1, which presumably represents the same genetic influence as the weaker QTL on chromosome 1 (LOD score 3.8, 49cM) in the single QTL analysis. Multiple QTL mapping also identified significant loci on chromosomes 3 and 8 for collateral number (LOD scores of 7 and 5, resp.), and interaction between the QTL on chromosomes 1 and 3 (LOD score 7). Suggestive QTL on chromosomes 6 and 10 were not confirmed. These results are summarized in Figure 2B; the inset shows the final model for collateral number. We have named the QTL according to convention by descending order of LOD score as *Canq1-4* (collateral artery number QTL), *Cadq1* (diameter), and *Cacq1-2* (“conductance”). Table 1 summarizes effect sizes, the modes of inheritance (additive or dominant) and their degree, and the statistical significance. We also detected slight segregation distortion between proximal chromosome 10 and distal chromosome 6 ($p<0.03$ by Chi-square test). One possible explanation for these findings is that linkage disequilibrium exists between the loci on chromosomes 6 and 10 and the major effect on chromosome 7, a condition controlled for by multiple QTL analysis.

Like the single QTL analysis, multiple QTL analysis failed to find any effect of *Vegfa*, *Fllt1*, or *Clic4*. To search exhaustively for potential epistases with these genes, we fixed all main effects and the interaction, then searched for interaction between *Canq1* and any other locus. No significant interaction was found (Online figure V).

To evaluate the genetic effects of the QTL on chromosome 7 for the 3 collateral traits, the average phenotype values were plotted against genotype for mice grouped by genotype at the marker nearest the peak, rs13479513. Mice homozygous for the B6 allele or heterozygous (B6-Bc) did not differ significantly from B6 or the F1 population, respectively, in any of the traits (Figure 3A, B). The Bc-Bc group also did not differ from the Bc parental in diameter. Thus, these phenotypes are largely determined by the single B6 allele when present. For collateral number, however, Bc-Bc F2 mice had significantly more pial collaterals than the parent Bc (3.9 vs. ≤0.5, $p<0.001$). The same is true of the derived parameter, “conductance” (56 conductance units vs. 12 for Bc, $p<0.05$). In addition, in our study of 15 inbred strains (18), Bc was significantly lower in pial collateral number than the two closest strains (Bc, 0.2 collaterals per hemisphere; SWR, 1.3, $p=0.0004$ vs. Bc; AKR, 1.7, $p<0.0001$ vs. Bc; Online figure I). These results suggest that additional loci, possibly unique to Bc among these strains, are responsible for the very low numbers of collaterals in Bc mice and are consistent with our finding of 3 additional QTL for collateral number but not diameter.

To see phenotypic effects, the genotype at a hypothetical marker located exactly at the peak of each of the QTL on chromosomes 1, 3 and 8 was imputed and the mice grouped according to these genotypes (Figure 3B). This shows that the QTL on chromosome 1 acts

in the same direction as that on chromosome 7 (ie, to favor greater number and conductance in B6; first and third panels in Figure 3B), while those on chromosomes 3 and 8 act in the other direction, albeit weakly (first panel).

The major effect of chromosome 7 is confirmed with chromosome substitution strains (CSS)

The inbred strain A/J is similar to Bc in haplotype structure under *Canq1*. It is also similar in hindlimb necrosis and recovery of hindlimb perfusion following femoral artery ligation (22) and infarct volume after MCAO (23) (see Discussion). These phenotypic characteristics, which gave a QTL in the same position as *Canq1*, were recapitulated in both of these studies in the strain C57BL/6J-Chr $7^{A/J}$/NaJ (CSS7), in which chromosome 7 in the B6 stain has been replaced by chromosome 7 from A/J. We therefore measured native collateral traits for CSS7. New data on A/J mice (n=8) in this study confirmed our previous results (18); A/J has 65% fewer pial collaterals than B6, and CSS7 is not statistically different from A/J (Figure 4A). CSS7 has slightly larger collateral diameter than Bc (12.6um vs. 8.6um for A/J, $p<0.003$), but diameter is substantially smaller than in B6 (12.6 vs. 24.6um for B6, $p<0.001$; Figure 4B). Similarly, CSS7 has 70% lower conductance than B6, compared to 86% lower for A/J and 98% lower for Bc (Figure 4C). Hence, CSS7 largely mimics Bc in all 3 native collateral traits, as it does for necrosis in hindlimb ischemia and cerebral infarct volume following MCAO (22,23). However, the significant difference between CSS7 and A/J for diameter and conductance and trend toward significance difference for number suggest that loci on additional A/J chromosomes influence collateral traits. Failure to find such evidence in previous studies using CSS7 analysis for recovery of hindlimb perfusion and necrosis score (22) and infarct volume (23) may arise because these downstream traits are removed from the underlying physiological mechanisms—that are dominated by native collateral extent and collateral remodeling.

Different amounts of cortical territory supplied by each of the main arteries (MCA, ACA, and PCA) are determinants of infarct volume after MCAO (18) and could, in principle, be determinants of pial collateral extent. And A/J mice have a larger percentage MCA territory that could potentially confound interpretation of the A/J and CSS7 data (18). Therefore, we also examined tree territories. The percentage MCA territory in CSS7 mice was not different from that of B6 and Bc mice (Figure 4D). In contrast, chromosome 17 (see below) transferred a significant part of the enlarged MCA territory phenotype of A/J to B6, consistent with the notion that loci on chromosomes other than 7 are responsible for the enlarged MCA tree in A/J mice. These data are consistent with our previous finding that collateral number and diameter show essentially no correlation with tree territory ($r^2=0.05$ and 0.01, resp) (18).

Since no QTL was found on chromosome 17 for collateral traits, cerebral infarct volume (23), or necrosis score and recovery of perfusion in a hindlimb ischemia model (22), CSS17 was also examined for pial collateral traits as a negative “control” to validate the CSS approach. CSS17 was not different from B6 in collateral number and conductance (Figure 4A, C). However, collateral diameter was significantly lower in CSS17 than in B6 (20um vs. 24.6um, $p<0.0002$), but it was still larger than in A/J by a substantial amount (20um vs. 8.6um, $p<0.0001$). These data suggest that the preparation of the CSS strains did not, per se, cause the Bc-like low values for native collateral traits found in CSS7, thereby reinforcing the conclusion that the main effect for low collateral number, diameter, and conductance resides on chromosome 7. The significant reduction in collateral diameter in CSS17 indicates that chromosome 17 of A/J mice harbors a genetic factor(s) that negatively affects this trait when introgressed onto the B6 background.

Importantly, the above findings offer a physiological basis for the previously identified QTL on chromosome 7 linked to hindlimb ischemia and cerebral infarct volume (22,23), ie, a gene variant(s) that confers variation in native collateral extent.

Cell-cell signaling and immune response pathway genes are enriched in *Canq1*

We subjected all genes in the Entrez database within the 95% confidence interval of *Canq1* (132.3–135.8) to Ingenuity pathway enrichment analysis (Ingenuity Systems, Redwood, CA). After adjustment for multiple-testing errors (Benjamini-Hochberg adjusted p value <0.05), enrichment was found for cell-cell signaling and immune response genes (Online Figure VI). These findings are supported by potential candidate genes responsible for variation in collateral extent revealed by association mapping (below).

Association mapping links pial collateral traits to a narrow region within *Canq1*

Given the strength of the QTL on chromosome 7, one can speculate that inbred strains that share haplotype identity with B6 will have a B6 collateral phenotype, and similarly for Bc. Thus, by comparing the structure within the region of the QTL across multiple inbred strains, it should be possible to narrow the region harboring the genetic element(s) responsible for the QTL. However, as extensively discussed by Kang et al. (21), the population structure and relatedness among inbred strains lead to high false positive rates and low statistical power. To circumvent these problems, we applied the efficient mixed model association (EMMA) algorithm designed by Kang et al. to the 134 individuals (8–10 per strain) of the 15 inbred strain set we studied previously (Online figure I;18). The relatedness among inbred strains was modeled as a random effect. The kinship matrix (covariance matrix) was calculated using densely imputed SNPs with confidence levels of ≥0.9 obtained from the Jackson Laboratory web site (http://phenome.jax.org/pub-gi/phenome/mpdcgi?rtn-snps/download). Upon interrogating each of the 41,000 SNPs in the 127–142Mb region on chromosome 7, a tight group of 18 SNPs at 132.356 to 132.529Mb was found to have the greatest significance (p=2.2x10E-5; Figure 5, group A). This narrow region overlaps the proximal boundary (132.4Mb) of the previously defined 95% confidence interval. This concordance strongly suggests that the 172 kb region harbors genetic variation that determines native collateral extent. Two predicted genes fall in this region (Table 2). Inclusion of the next most significant set of SNPs (p<4.2×10E-4; Figure 5, group B), expands the region telomerically to 132.817, to include a total of 9 genes (Table 2).

LOD score profiling for collateral remodeling identifies a QTL on chromosome 11

Obstruction of the trunk of a main artery tree cross-connected to an adjacent tree by collaterals, as in MCAO, induces sustained unidirectional flow and shear stress in the collaterals (14). This induces the collateral vessels to increase their lumen diameter and wall thickness, a process called outward remodeling or arteriogenesis that can be quantified as a fold change in diameter in the operated hemisphere relative to the non-operated hemisphere (5). We showed that in mice this process occurs during the first few days after MCAO, and that the amount of remodeling is subject to strong genetic influence (18). Herein, we examined remodeling 6 days after MCAO because at this time remodeling had reached a maximum in B6 mice but was considerably less in Bc (18). A genome-wide scan using the single-QTL model for fold change revealed a significant QTL identical to *Canq1* and a weaker QTL on chromosome 10 (Figure 6) The relationship between velocity and cross-sectional area proscribes that larger diameter collaterals will have lower fluid shear stress after ligation (eg MCAO), leading to less shear-induced remodeling. In support of this, a highly significant inverse correlation was obtained for collateral remodeling and baseline diameter (Figure 6), in agreement with previous results (18). Hence, diameter is a covariate for remodeling. When set as such in the statistical model, the QTL on chromosomes 7 and

10 were lost, and a significant QTL on chromosome 11 (LOD score 3.5) was obtained (Figure 6, blue curve; Table 1). These results are consistent with the expectation that genes regulating collateral formation (ie, native number and diameter) in the embryo (14) are likely to differ from those regulating remodeling in the adult (6).

Discussion

This study sought to identify the genetic determinants responsible for the wide variation in the number and diameter of native (pre-existing) collaterals in healthy tissue of inbred mice (6,14–20) and potentially in humans (7–13), and collateral remodeling after arterial occlusion (14,16). We recently reported that these traits in the brain vary widely with genetic background, with C57BL/6 (B6) and BALB/c (Bc) mice being at the two extremes, and that this variation strongly correlates with infarct volume (18). In the present study, we performed genome-wide linkage analysis in an F2 cross between B6 and Bc mice using collateral number, diameter and conductance as quantitative traits and identified a major locus on chromosome 7 that modulates collateral extent. Further evidence for the involvement of this locus was supported by use of chromosome substitution strains. We also identified a locus on chromosome 11 for collateral remodeling after setting the diameter at baseline as a covariate. High density association mapping was then used to narrow down the chromosome 7 QTL to a 172 kb region containing 9 candidate genes. Importantly, the major QTL on chromosome 7 is at the same locus as a previously reported QTL linked to hindlimb ischemia (22) and cerebral infarct volume (23). This identification of a common QTL on chromosome 7 is very robust, having been made for physiologically linked but quite distinct phenomena (native collateral extent, cerebral infarct volume and hindlimb necrosis/perfusion recovery) in multiple tissues (cerebral pial circulation, cerebral cortex and skeletal muscle). In the previous papers, the underlying physiological basis was not identified. The present findings strongly suggest that that physiological basis is genetically determined variation in native collateral extent. As such, our results focus attention on the possibility that a major component of the amount of tissue injury in response to arterial obstruction in the brain, heart and peripheral limbs may be a person's genetic predisposition influencing the extent of the collateral circulation.

In the study by Dokun et al (22), the magnitudes of necrosis score and recovery of perfusion assessed 21 days after femoral artery ligation depended in large part on both collateral extent and collateral remodeling, although additional mechanisms could contribute (1–6,16–20). However, infarct volume assessed 24 hours after MCAO (23), when only minimal remodeling of pial collaterals could have occurred, depends to a larger degree on native collateral extent. Given the dependence of shear stress-induced remodeling on collateral diameter, our results argue strongly that variation in native collateral extent exerted by the chromosome 7 locus is the major biological substrate underlying both previously reported QTL (22,23). This also provides a physiological mechanism—collateral formation during the perinatal period—on which to prioritize candidate genes and genetic elements for known or suspected involvement. Furthermore, since B6 and Bc strains have high and low native collateral extent, respectively, in pia, skeletal muscle, and intestine (16), these results suggest that the same genetic determinants will apply to variation in collateral function in other tissues.

Infarct volume is inversely related to the prevailing arterial pressure after cerebral artery occlusion (since arterial pressure is the driving force for collateral perfusion), which could potentially impact interpretation of our results. As previously noted by Keum and Marchuk for Civq1 (23), the centromeric tail of Canq1 overlaps the telomeric end of a syntenic rat chromosome 1 locus for blood pressure and infarct volume (24). However, Yao et al (24) found that stroke-prone, spontaneously hypertensive rats (SPSHR) made congenic for this

locus from the normotensive WKY rat showed both lower blood pressure and smaller cerebral infarct volumes after MCAO. The latter effect is *opposite* to what is expected, suggesting that secondary changes in vascular structure, smooth muscle tone or pressure-independent genetic factors also linked to the rat locus might instead be involved (24). In addition, the location of the telomeric end of the introgressed piece corresponds to 128 Mb in mouse chromosome 7, which is well upstream of the peaks suggested by EMMA and the multiple QTL analysis. Finally, arterial pressures in Bc and B6 mice are virtually identical, whether measured in the anesthetized or conscious state (25–28). Thus, these findings do not support arterial pressure differences as a physiological mechanism underlying the common QTL identified on chromosome 7 in the present or previous studies (22,23).

Majid et al. (29) found no significant difference in blood flow velocity between the B6 and Bc strains measured with a laser Doppler probe in an estimated $1mm^3$ of tissue in the "core of the MCA ischemic territory" 10 minutes after MCAO, and concluded that non-hemodynamic variables (ie, including no differences in collateral extent) are responsible for the different infarct volumes in the two strains. However, several considerations call this conclusion into question: Values trended lower for the Bc mice. The Doppler probe that was used measures velocity rather than flow; velocity can remain unchanged despite reduced flow if diameter also declines (eg, by passive collapse after MCAO), measurement of overall cerebral blood flow velocity in the MCA territory from a single-point probe is unreliable (eg, 24). Lastly, the Doppler signal includes blood flow in the dura mater, which is not supplied by the MCA.

Canq1, *LSq-1* (22) and *Civq1* (23) are broad loci that contain many genes. The gene list under *LSq-1* was reduced by interval-specific haplotype association mapping based on the criterion that haplotypes under the QTL would be identical in Bc and A/J mice and different from B6 (22). For cerebral infarct volume (*Civq1*), the criterion was expanded to include strain SWR, further reducing the list of candidate genes to only 12 in a 10 Mb region, from 132.47 (49334400M02RIK) to 142.37 Mb (Dock1) (23). These analyses also apply to *Canq1*. However, to further refine this region we applied the recently described efficient mixed model association method (EMMA; 21) to 41,000 known, high quality SNPs in the 15 Mb region. Low statistical power and high false-positive rate can arise in haplotype mapping in mice due to genome-wide application, limited sample size, and lack of control for population structure (21). Therefore, we confined our association mapping to 127–142 Mb (*Canq1*) and native collateral number from 15 inbred strains (n=8–10 of each strain; 18). We also used dense markers to infer with high probability ($p \geq 0.9$) missing markers as identical-by-descent among the 15 inbred strains. Finally, we applied the resultant kinship matrix to the EMMA algorithm to model population structure as a random effect to account for the population structure problem. This analysis pointed to a narrow region encompassing 9 genes, of which 7 failed to satisfy the haplotype criterion applied by Dokun et al. and by Keum and Marchuk. Thus, only one gene (4933440M02RIK, a predicted gene with EST support but no annotation) is common to the list of Keum and Marchuk and the list suggested by EMMA. There are no known miRNAs in the high-probability 9-gene EMMA region, nor is it known whether other classes of regulatory DNA or RNA elements (eg, long non-coding RNAs) are present. Future work will be needed to identify the genetic element(s) underlying the major QTL on chromosome 7 and to define the molecular pathways controlling collateral formation in the embryo and thus the wide variation in the adult.

Several genes with known influences on native collateral extent or collateral remodeling were not detected in our analysis. Experiments using mice haplo-insufficient or null for *Vegfa*, *Flt1* (VEGFR1) and *Clic4*, have shown that these molecules are strong positive determinants of perinatal collateral formation and maturation and thus native collateral

number and diameter in the adult (19; Lucitti and Faber, unpublished data; 20). Furthermore, induction of VEGF-A expression is significantly lower in Bc compared to B6 (14,16,19,30,31) (expression of Flt1 and CLIC4 have not been examined in Bc versus B6). However, we found no QTL in the regions of these genes in either single or multiple QTL analysis. In addition, no interaction between *Canq1* and any other locus was found when all main effects and the epistasis between *Canq2* and *Canq3* were fixed. This outcome was expected for *Vegfa* and *Clic4*, since these genes and their flanking sequences are essentially identical in B6 and Bc. The Flt1 gene and flanking sequences are different between B6 and Bc, and are identical in Bc and A/J. However, whether this has functional consequences in the context of the B6 and Bc backgrounds is not known. One or more of the genetic elements underlying *Canq1-Canq4* may act in a weak *trans* manner to influence expression of VEGF-A, Flt1 or CLIC4, or other molecules involved in collateral formation may compensate for deficiencies in this pathway in Bc mice. Additional studies will be required to determine the role(s) of variants underlying the QTL identified in the present study.

Ingenuity pathway analysis within the 95% confidence interval of *Canq1* found enrichment for immune response genes, and IL4 receptor alpha and IL21 receptor were among the 9 genes in the high significance region identified by EMMA association mapping. While collateral remodeling is known to be highly dependent on the immune system (1–5), no studies have examined whether collateral formation and maturation during the perinatal period, which determine native collateral number in the adult, involve immune cell function. Van Weel et al. (32) found evidence suggesting involvement of the known difference in natural killer cell (NKC) function in B6 versus Bc mice—associated with a different haplotype on distal chromosome 6 involving the NKC gene complex locus (33)—in the difference in recovery of blood flow after femoral artery ligation in these strains (which is dependent, in large part, on native collateral extent and collateral remodeling). However, this group recently reported, using congenic mice with this locus introgressed into the opposite strain, that the difference in native collateral number does not depend on the NKC locus (34). This is consistent with our finding of no QTL on distal chromosome 6. It also is consistent with lack of agreement of this chromosome 6 haplotype in 8 inbred mouse strains with native collateral number in these same strains (18,34). Our results linking variation in remodeling of pial collaterals to its dependence on initial collateral diameter and thus the chromosome 7 locus, plus the diameter-independent locus on chromosome 11, are not congruent with a role for chromosome 6 in collateral remodeling. Van Weel et al did not examine if mice congenic for the chromosome 6 NKC locus show transference of differences in the remodeling phenotype.

We identified different genetic architectures for variation in collateral number, diameter and collateral remodeling. Native collateral number and diameter in young adult mice (eg, 10 week-old as studied herein) are determined by two processes—collateral formation which occurs late embryonically after the general circulation has formed—and collateral maturation which occurs during the first three postnatal weeks (14). The former involves sprouting of a unique plexus of arterial-fated endothelial cell tubes, while the latter involves pruning away of a portion of these nascent collaterals, followed by lumen enlargement and smooth muscle cell investment of those that are retained (6,14). Collateral remodeling, which occurs in obstructive disease in the adult, involves a complex signaling and restructuring process (1–5). Although much is known about the molecular signaling pathways directing collateral remodeling, almost nothing is known about those directing formation and maturation (6). The very different mechanisms and times of occurrence of the three processes suggest they are guided, at least in part, by genes unique to each. In support of this, collateral number and diameter shared a common QTL (*Canq1*), while number was linked to three additional QTL, and a QTL for remodeling was found on chromosome 11. In addition, collateral number, diameter and amount of remodeling have unique rank-orders

among 15 inbred strains (18). Importantly, all three traits are critical determinants of the severity of stroke and ischemic disease of the heart and other tissues (6).

In conclusion, our findings show that the extent and remodeling of the native collateral circulation is subject to wide variation that is due, primarily, to a remarkably strong polymorphism on chromosome 7, with smaller contributions from several additional QTL. These findings provide the underlying physiological basis for a recently reported QTL at the same locus on chromosome 7 linked to severity of hindlimb ischemia and cerebrovascular stroke (22,23). Variation in collateral traits reflect yet-to-be identified genetic and environmental factors that impact formation and maturation of collaterals, maintenance of them during natural growth to adulthood and subsequent aging, and collateral remodeling in obstructive disease. Our findings establish a foundation for future studies to identify the alleles and molecular pathways that direct these processes and account for their wide variability among healthy individuals, with obvious implications for patient evaluation and management.

Novelty and Significance

What is Known?

- Most tissues have a collateral circulation composed of a small number of native pre-existing “endogenous bypass vessels” interconnecting adjacent arterial trees, whose extent (density and diameter) is a critical determinant of the severity of tissue injury in obstructive diseases such as stroke, coronary artery disease and peripheral artery disease.
- The extent of native pre-existing collaterals (ie, conductance of the collateral circulation), plus their amount of lumen enlargement (growth/remodeling) in obstructive disease, exhibit remarkably wide variation dependent in part on differences in genetic background.
- The genetic loci responsible for variation in native collateral extent or collateral remodeling induced by arterial obstruction have not been identified.

What New Information Does This Article Contribute?

- The cerebral collateral circulation and its response to middle cerebral artery occlusion in in-bred mouse strains was used to identify four quantitative trait loci (QTL) that together comprise the majority of the heritable difference in native collateral extent; a different QTL was identified for variation in collateral remodeling.
- Association mapping narrowed the potential candidate genes from ~300 to 9 within the main locus on chromosome 7.

The native density and diameter of collaterals, as well as their outward remodeling in obstructive disease (arteriogenesis), vary widely—in part due to unknown genetic factors. We show that in mice this genetic variation maps to a remarkably strong polymorphism on chromosome 7. Moreover, our findings provide the underlying physiological basis for a recently reported QTL at the same locus linked to differences in severity of limb ischemia and stroke. Variation in collateral extent in tissues reflects yet-to-be identified genetic and environmental factors that impact the formation and the maintenance of these vessels. Our findings provide a foundation for future studies to identify the alleles and molecular pathways that direct these processes and account for their wide variability among even healthy individuals. Such knowledge may permit stratification of patients according to collateral extent for treatment with arteriogenic therapies, in clinical trials to assess new arteriogenic therapies, and in assessment of risk severity for stroke,

myocardial infarction and peripheral artery disease. This new understanding may also lead to novel therapies to promote formation of new collaterals in patients with collateral circulatory insufficiency.

Supplementary Material

Refer to Web version on PubMed Central for supplementary material.

Non-standard abbreviations and acronyms

B6	C57BL/6J strain of inbred mice
Bc	BALB/cByJ strain of inbred mice
A/J	A/J strain of inbred mice
Chr	chromosome
CSS7	Chr substitution strain 7--A/J mice with Chr 7 of B6 strain introgressed in place of the A/J Chr 7
CSS17	Chr substitution strain 17--A/J mice with Chr 17 of B6 strain introgressed in place of the A/J Chr 17
QTL	quantitative trait locus
SNP	single nucleotide polymorphism
LOD	Logarithm of the odds
cM	centiMorgans
Mb	megabase pairs
MCAO	middle cerebral artery occlusion
ACA	anterior cerebral artery
PCA	posterior cerebral artery
EMMA	efficient mixed model association algorithm

Acknowledgments

We thank Drs. Timothy Wiltshire and Oscar Suzuki (UNC) for assistance with help in marker refinement, and Drs. Wiltshire, Daniel Pomp and Fei Zou (UNC) for their discussions.

Sources of Funding

NIH grants HL62584 and HL090655 (JEF).

References

1. Sherman JA, Hall A, Malenka DJ, De Muinck ED, Simons M. Humoral and cellular factors responsible for coronary collateral formation. Am J Cardiol. 2006; 98:1194–1197. [PubMed: 17056326]
2. Grundmann S, Piek JJ, Pasterkamp G, Hoefer IE. Arteriogenesis: basic mechanisms and therapeutic stimulation. Eur J Clin Invest. 2007; 37:755–766. [PubMed: 17764463]
3. Kinnaird T, Stabile E, Zbinden S, Burnett MS, Epstein SE. Cardiovascular risk factors impair native collateral development and may impair efficacy of therapeutic interventions. Cardiovasc Res. 2008; 78:257–264. [PubMed: 18178573]

4. Schirmer SH, van Nooijen FC, Piek JJ, van Royen N. Stimulation of collateral artery growth: traveling further down the road to clinical application. Heart. 2009; 95:191–197. [PubMed: 19144878]
5. Schaper W. Collateral circulation: past and present. Basic Res Cardiol. 2009; 104:5–21. [PubMed: 19101749]
6. Faber, JE.; Dai, X.; Lucitti, J. Ch 1, Genetic and environmental mechanisms controlling formation and maintenance of the native collateral circulation. In: Diendl, E.; Schaper, W., editors. Arteriogenesis. 2010. p. 3-32.(in press)
7. Meier P, Gloekler S, Zbinden R, Beckh S, de Marchi SF, Zbinden S, Wustmann K, Billinger M, Vogel R, Cook S, Wenaweser P, Togni M, Windecker S, Meier B, Seiler C. Beneficial effect of recruitable collaterals: a 10-year follow-up study in patients with stable coronary artery disease undergoing quantitative collateral measurements. Circulation. 2007; 116:975–983. [PubMed: 17679611]
8. Bang OY, Saver JL, Buck BH, Alger JR, Starkman S, Ovbiagele B, Kim D, Jahan R, Duckwiler GR, Yoon SR, Vinuela F, Liebeskind DS. Impact of collateral flow on tissue fate in acute ischaemic stroke. J Neurol Neurosurg Psychiatry. 2008; 79:625–629. [PubMed: 18077482]
9. Christoforidis GA, Karakasis C, Mohammad Y, Caragine LP, Yang M, Slivka AP. Predictors of hemorrhage following intra-arterial thrombolysis for acute ischemic stroke: the role of pial collateral formation. AJNR Am J Neuroradiol. 2009; 30:165–170. [PubMed: 18768718]
10. Miteff F, Levi CR, Bateman GA, Spratt N, McElduff P, Parsons MW. The independent predictive utility of computed tomography angiographic collateral status in acute ischaemic stroke. Brain. 2009; 132:2231–2238. [PubMed: 19509116]
11. Maas MB, Lev MH, Ay H, Singhal AB, Greer DM, Smith WS, Harris GJ, Halpern E, Kemmling A, Koroshetz WJ, Furie KL. Collateral vessels on CT angiography predict outcome in acute ischemic stroke. Stroke. 2009; 40:3001–3005. [PubMed: 19590055]
12. Abul-Khoudoud O. Diagnosis and risk assessment of lower extremity peripheral arterial disease. J Endovasc Ther. 2006; 13 Suppl 2:II10–II18. [PubMed: 16472008]
13. Bobek V, Taltynov O, Pinterova D, Kolostova K. Gene therapy of the ischemic lower limb--Therapeutic angiogenesis. Vascul Pharmacol. 2006; 44:395–405. [PubMed: 16698324]
14. Chalothorn D, Faber J. Formation and maturation or the murine native cerebral collateral circulation. J Molec Cell Cardiol. 2010 Mar 25. Epub ahead of print.
15. Helisch A, Wagner S, Khan N, Drinane M, Wolfram S, Heil M, Ziegelhoeffer T, Brandt U, Pearlman JD, Swartz HM, Schaper W. Impact of mouse strain differences in innate hindlimb collateral vasculature. Arterioscler Thromb Vasc Biol. 2006; 26:520–526. [PubMed: 16397137]
16. Chalothorn D, Clayton JA, Zhang H, Pomp D, Faber JE. Collateral density, remodeling, and VEGF-A expression differ widely between mouse strains. Physiol Genomics. 2007; 30:179–191. [PubMed: 17426116]
17. Zbinden S, Clavijo LC, Kantor B, Morsli H, Cortes GA, Andrews JA, Jang GJ, Burnett MS, Epstein SE. Interanimal variability in preexisting collaterals is a major factor determining outcome in experimental angiogenesis trials. Am J Physiol Heart Circ Physiol. 2007; 292:H1891–H1897. [PubMed: 17189353]
18. Zhang H, Prabhakar P, Sealock RW, Faber JE. Wide genetic variation in the native pial collateral circulation is a major determinant of variation in severity of stroke. J Cere Blood Flow Metab. 2010; 30:923–934.
19. Clayton JA, Chalothorn D, Faber JE. Vascular endothelial growth factor-A specifies formation of native collaterals and regulates collateral growth in ischemia. Circ Res. 2008; 103:1027–1036. [PubMed: 18802023]
20. Chalothorn D, Zhang H, Smith JE, Edwards JC, Faber JE. Chloride intracellular channel-4 is a determinant of native collateral formation in skeletal muscle and brain. Circ Res. 2009; 105:89–98. [PubMed: 19478202]
21. Kang HM, Zaitlen NA, Wade CM, Kirby A, Heckerman D, Daly MJ, Eskin E. Efficient control of population structure in model organism association mapping. Genetics. 2008; 178:1709–1723. [PubMed: 18385116]

22. Dokun AO, Keum S, Hazarika S, Youngun L, Lamonte GM, Wheeler F, Marchuk DA, Annex BH. A QTL (LSq-1) on mouse chromosome 7 is linked to the absence of tissue loss following surgical hind-limb ischemia. Circulation. 2008; 117:1207–1215. [PubMed: 18285563]

23. Keum S, Marchuk DA. A locus mapping to murine chromosome 7 determines infarct volume in a mouse model of ischemic stroke. Circ Cardiovasc Genet. 2009; 2:591–598. [PubMed: 20031639]

24. Yao H, Cui Z-H, Masuda J, Nabika T. Congenic removal of a QTL for blood pressure attenuates infarct size produced by middle cerebral artery occlusion in hypertensive rats. Physiol Genomics. 2007; 30:69–73. [PubMed: 17327494]

25. Ryan MJ, Didion SP, Davis DR, Faraci FM, Sigmund CD. Endothelial dysfunction and blood pressure variability in selected inbred mouse strains. Arterioscler Thromb Vasc Biol. 2002; 22:42–48. [PubMed: 11788459]

26. Deschepper CF, Olson JL, Otis M, Gallo-Payet N. Characterization of blood pressure and morphological traits in cardiovascular-related organs in 13 different inbred mouse strains. J Appl Physiol. 2004; 97:369–376. [PubMed: 15047670]

27. Campen MJ, Tagaito Y, Jenkins TP, Balbir A, O'Donnell CP. Heart rate variability responses to hypoxic and hypercapnic exposures in different mouse strains. J Appl Physiol. 2005; 99:807–813. [PubMed: 15890760]

28. Zuurbier CJ, Emons VM, Ince C. Hemodynamics of anesthetized ventilated mouse models: aspects of anesthetics, fluid support, and strain. Am J. Physiol Heart Circ Physiol. 2002; 282:H2099–H2105. [PubMed: 12003817]

29. Majid A, He YY, Gidday JM, Kaplan SS, Gonzales ER, Park TS, Fenstermacher JD, Wei L, Choi DW, Hsu CY. Differences in vulnerability to permanent focal cerebral ischemia among 3 common mouse strains. Stroke. 2000; 31:2707–2714. [PubMed: 11062298]

30. Ward NL, Moore E, Noon K, Spassil N, Keenan E, Ivanco TL, LaManna JC. Cerebral angiogenic factors, angiogenesis, and physiological response to chronic hypoxia differ among four commonly used mouse strains. J Appl Physiol. 2007; 102:1927–1935. [PubMed: 17234796]

31. Vasquez-Pinto LM, Landgraf RG, Bozza PT, Jancar S. High vascular endothelial growth factor levels in NZW mice do not correlate with collagen deposition in allergic asthma. Int Arch Allergy Immunol. 2007; 142:19–27. [PubMed: 17016055]

32. Van Weel V, Toes REM, Seghers L, Deckers MML, de Vries MR, Eilers PH, Sipkens J, Schepers A, Eefting D, van Hinsbergh VWM, van Bockel JH, Quax PHA. Natural killer cells and $CD4^+$ T-cells modulate collateral artery development. Atheroscler Thromb Vasc Biol. 2007; 27:2310–2318.

33. Brown MG, Scalzo AA. NK gene complex dynamics and selection for NK cell receptors. Semin Immunol. 2008; 20:361–368. [PubMed: 18640056]

34. Taherzadeh Z, VanBavel E, de Vos J, Matlung HL, van Montfrans G, Brewster LM, Seghers L, Quax PH, Bakker EN. Strain-dependent susceptibility for hypertension in mice resides in the natural killer gene complex. Am J Physiol Heart Circ Physiol. 2010; 298:H1273–H1282. [PubMed: 20154263]

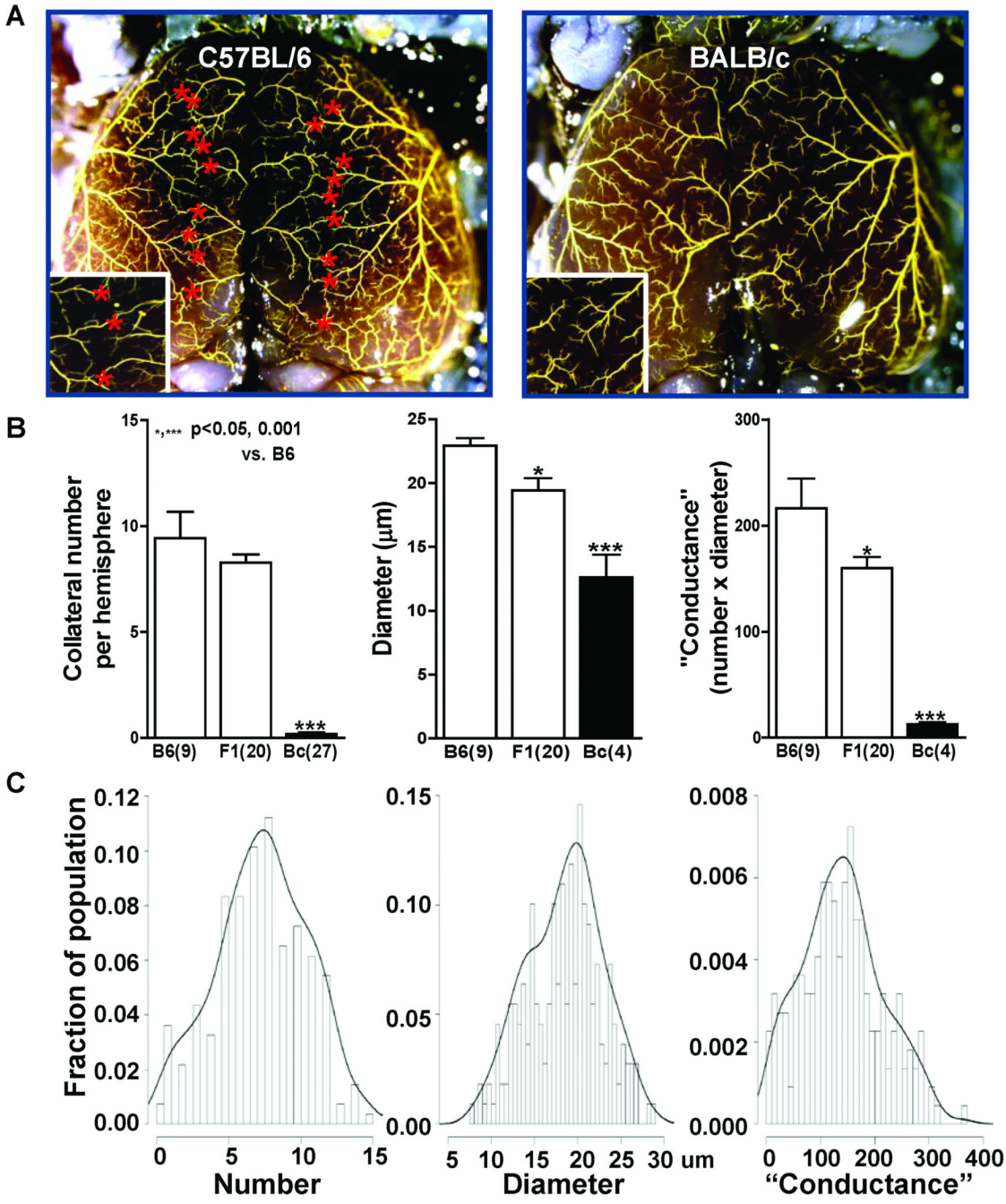

Figure 1. Phenotypes of the native cerebral cortical pial collateral circulation in C57BL/6 (B6), BALB/c (Bc), F1 and F2 mice

A, Mouse pial arterial circulation in B6 (left) and Bc (right) after clearing, dilating, and filling with yellow Microfil™ restricted from capillary transit. Collaterals cross-connecting the ACA and MCA trees in B6 are indicated (*). The Bc brain that is shown has no MCA-ACA collaterals. **B,** Number, diameter and "conductance" (number × diameter) of collaterals compared for B6, Bc and F1 mice. Data are given as mean ± SEM, with (n) = number of mice studied in this and subsequent figures unless indicated otherwise. The small n-size for Bc diameter and conductance reflects the large number of individuals in this strain with no

collaterals. **C,** Distributions and density curves for number per hemisphere, diameter, and conductance of collaterals of the F2 cohort (n=221).

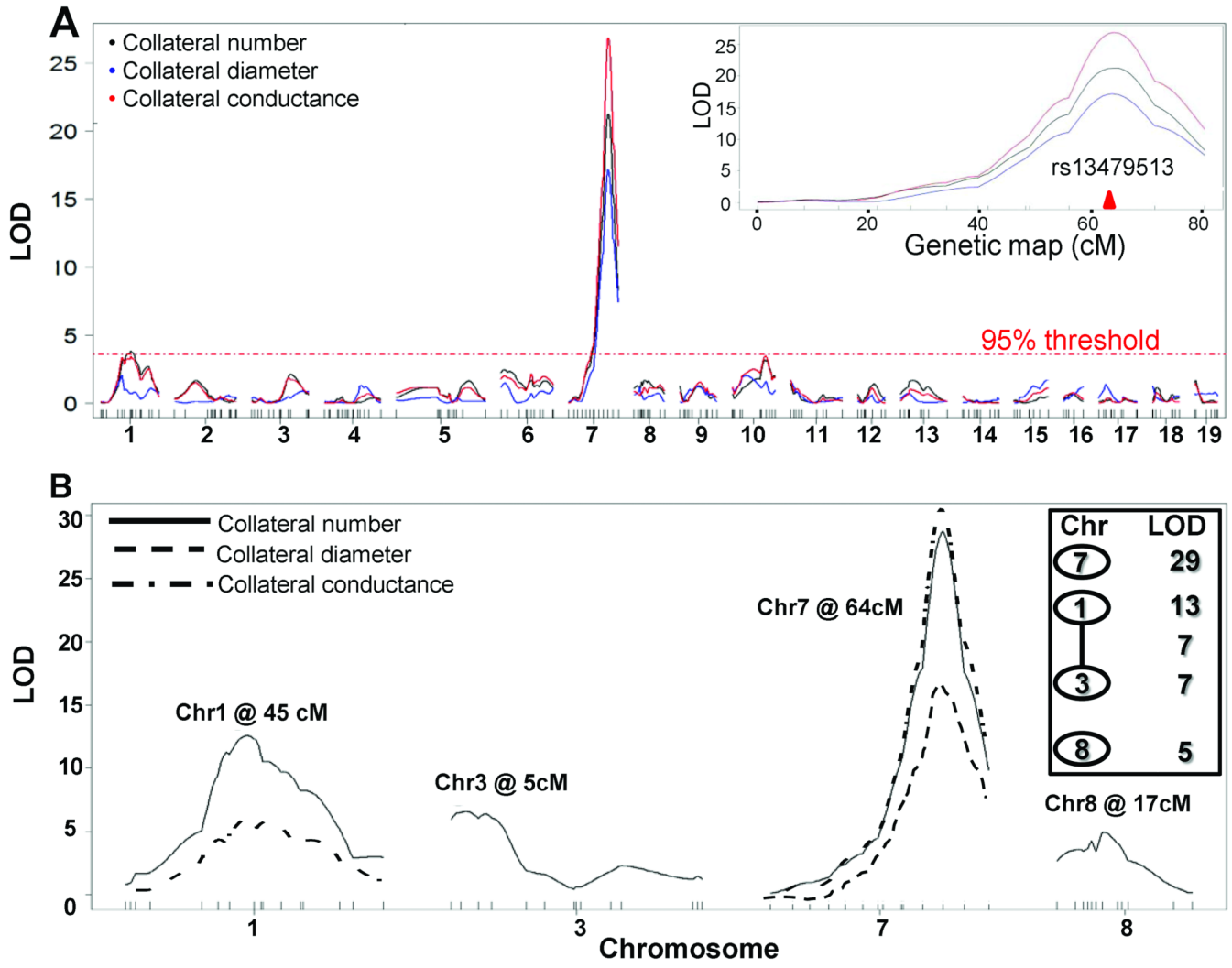

Figure 2. Genome-wide mapping of collateral traits in 221 F2 mice

A, LOD profiling using the single QTL model. Locations of genotyping SNPs are shown as ticks on the abscissa. 95% confidence level (dashed line) was estimated using 1000 permutations. Inset, higher resolution genetic map of the peak on chromosome 7. The location of the marker nearest the peak is indicated (triangle). **B,** LOD profiling using the multiple QTL model. Significant QTLs were found on chromosomes 1, 3, 7, and 8 for number (black line), on chromosome 7 for diameter (dashed line), and on chromosomes 1 and 7 for conductance (dot-dash line). Inset, schematic of the multiple QTL model for collateral number having the highest LOD. The solid line denotes interaction between the QTLs on chromosomes 1 and 3 (LOD score 7).

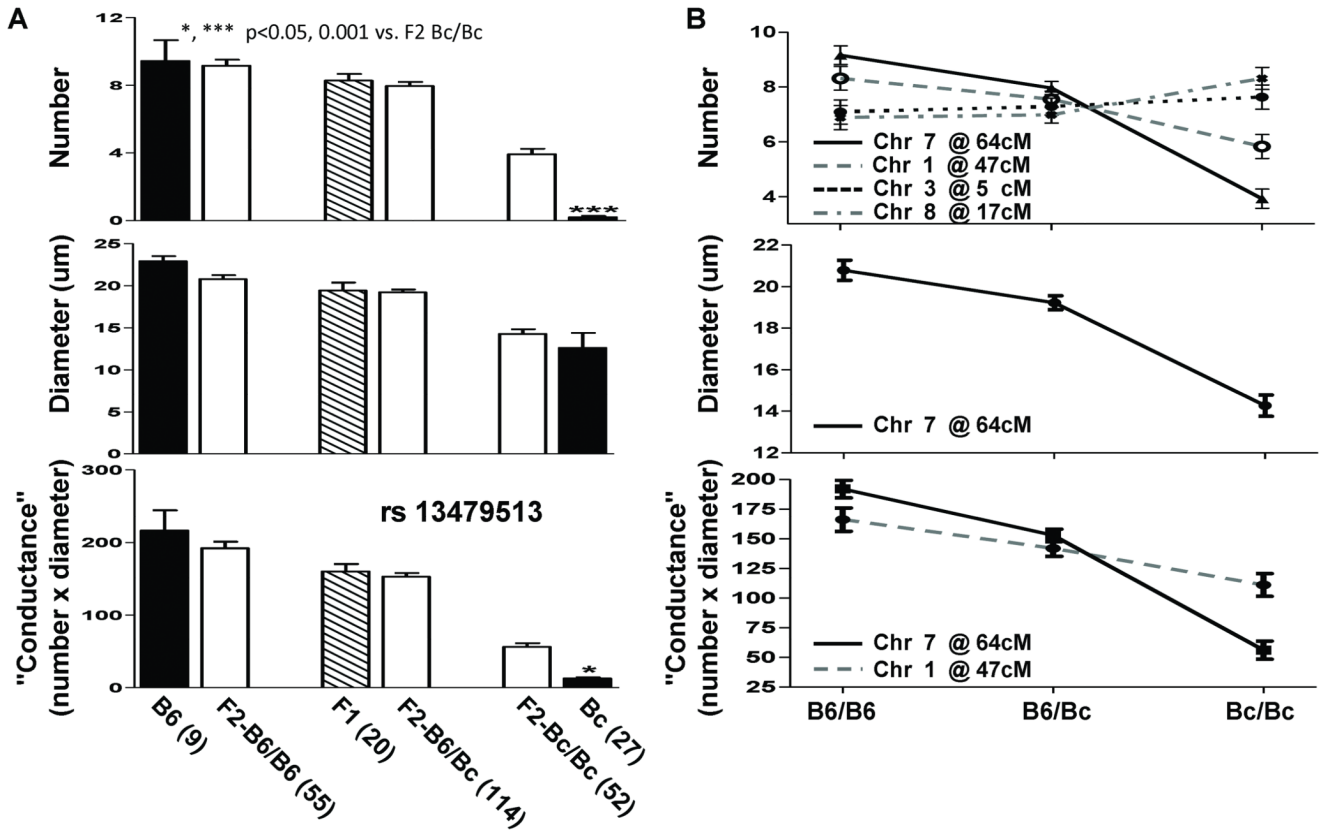

Figure 3. Influence of identified QTL on collateral traits

A, Phenotypic effects of the chromosome 7 QTL. Collateral number, diameter and conductance of parental, F1 and F2 mice grouped according to genotype at marker rs13479513 (see Fig. 1 inset). F2-B6/B6 mice and F2-B6/Bc mice are similar to parental B6 and F1 mice, resp., in all 3 traits. F2-Bc/Bc mice are similar to Bc in diameter (middle panel). These suggest that the chromosome 7 QTL accounts for the major difference in collateral number between B6 and Bc. However, F2-Bc/Bc mice are significantly different from Bc in collateral number and conductance, suggesting that additional loci must act with the chromosome 7 QTL to cause the very low collateral number in Bc mice. **B,** Phenotypic effects of the QTL identified by multiple QTL mapping. For each trait and QTL, F2 mice were grouped by genotype at the imputed peak SNP (see Supplemental Methods) and the average for each group plotted vs. genotype (see text).

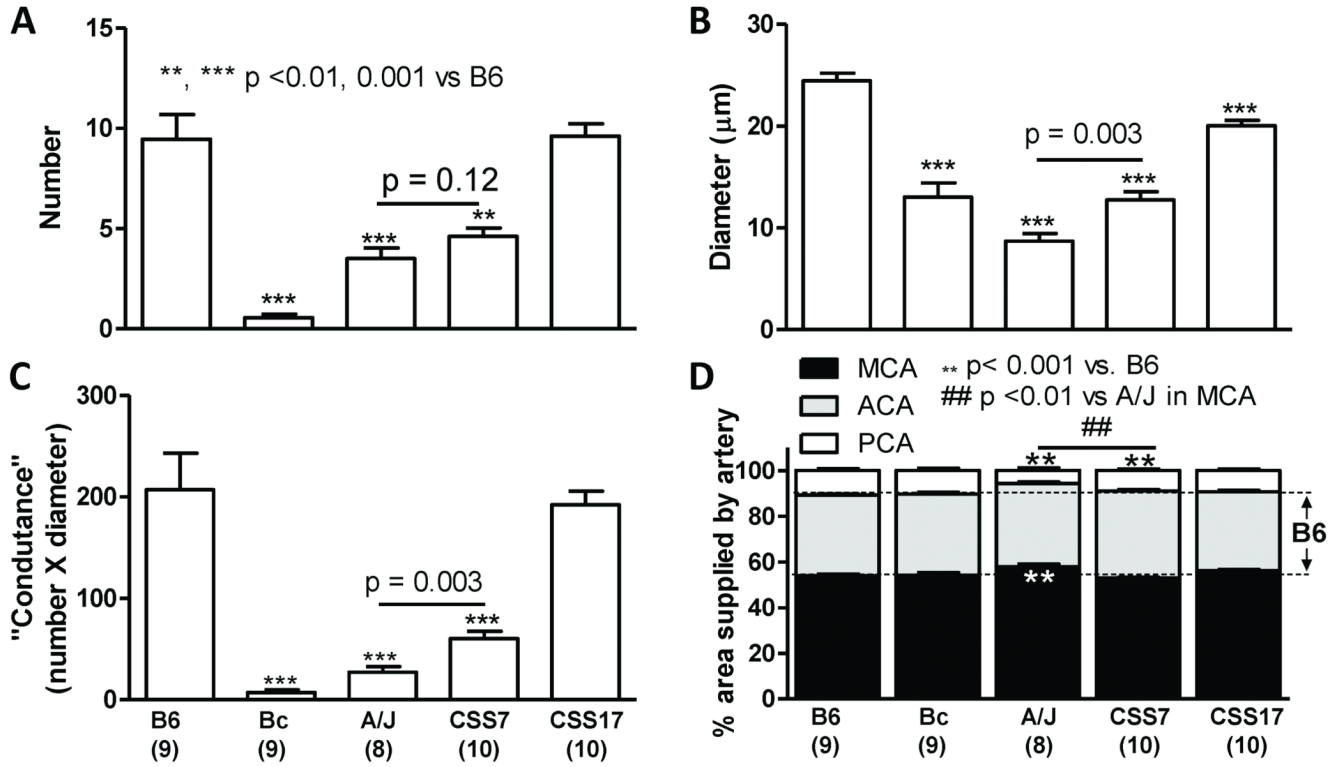

Figure 4. Chromosome substitution strains confirm a major effect of chromosome 7

A–C, Collateral extent traits in B6, Bc, A/J, CSS7 and CSS17 mice. A/J and Bc are similarly different from B6 in number and diameter ($p<0.001$; confirms Zhang et al. (18)) and in conductance. CSS7 mice (chromosome 7 in B6 replaced by chromosome 7 from A/J) are not different from A/J in number but are significantly different ($p<0.003$) from A/J in diameter and "conductance". Nonetheless, the replacement transfers most of the B6-A/J difference in each trait. In CSS17, intended as a negative control for validation of the CSS7 approach, collateral number is unchanged from B6 but diameter is modestly reduced. **D**, Fractions of the cerebral cortex area (territories) supplied by the ACA, MCA, and PCA. B6 and Bc have identical territories (confirms Zhang et al. (18)), while in A/J the MCA is slightly larger and the PCA correspondingly smaller than in B6. This difference is not transferred to CSS7, confirming the dissociation of collateral and cerebral artery tree territory phenotypes among inbred mouse strains (18).

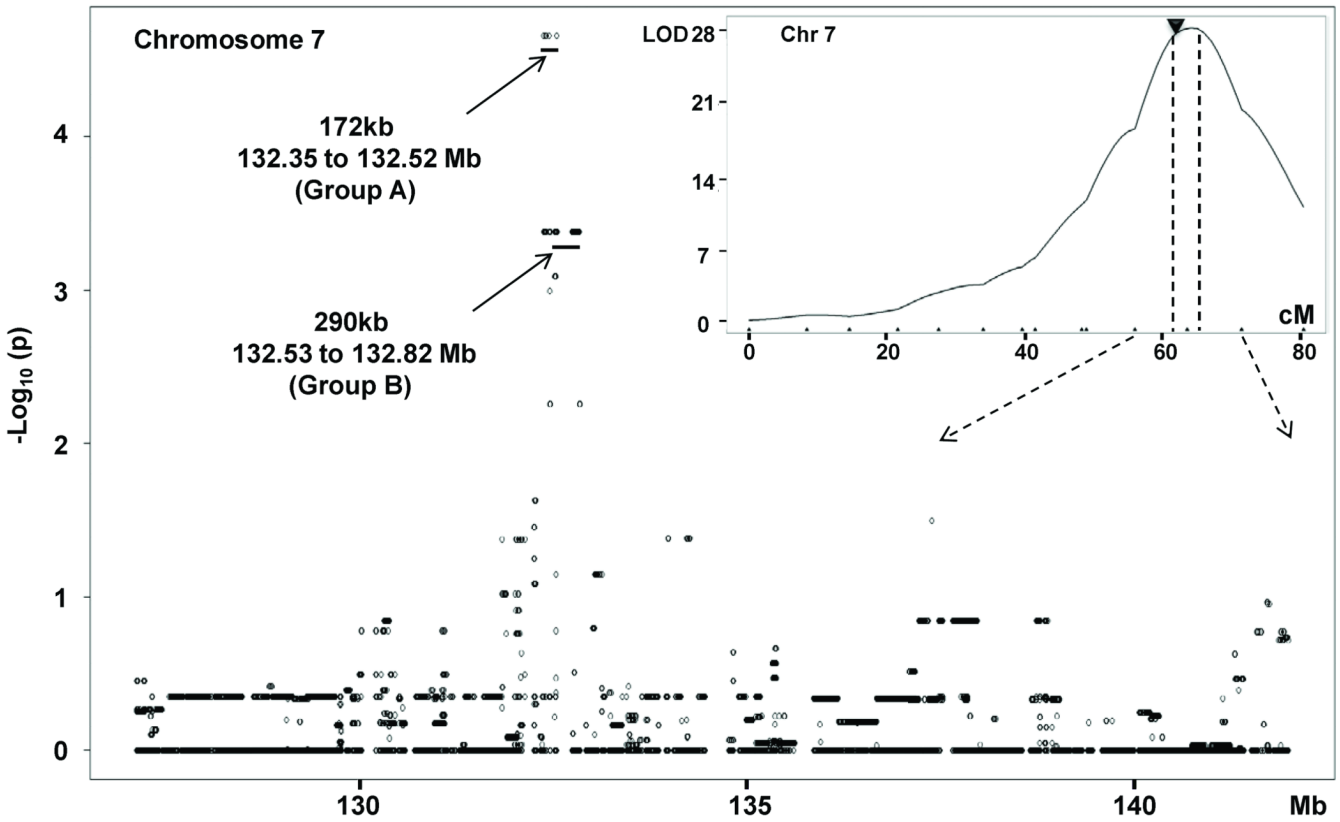

Figure 5. Highly significant region within *Canq1* identified by association mapping for native collateral number

The EMMA algorithm (21) was applied to collateral trait values in the 134 individuals of the 15 strain data of Zhang et al. (18) and the 41,000 high quality imputed SNPs under the *Canq1* peak (127 to 143 Mb; cM shown in the inset). A highly significant group of 18 SNPs (p=2.2E-5, Group A) slightly proximal to the QTL peak resulted (inset, black triangle). The second most significant group (155 SNPs, p=4.17E-4; Group B) spans a 290kb region. The genes in these groups are shown in Table 2. The vertical dashed lines in the insert delimit the 95% confidence interval of *Canq1*.

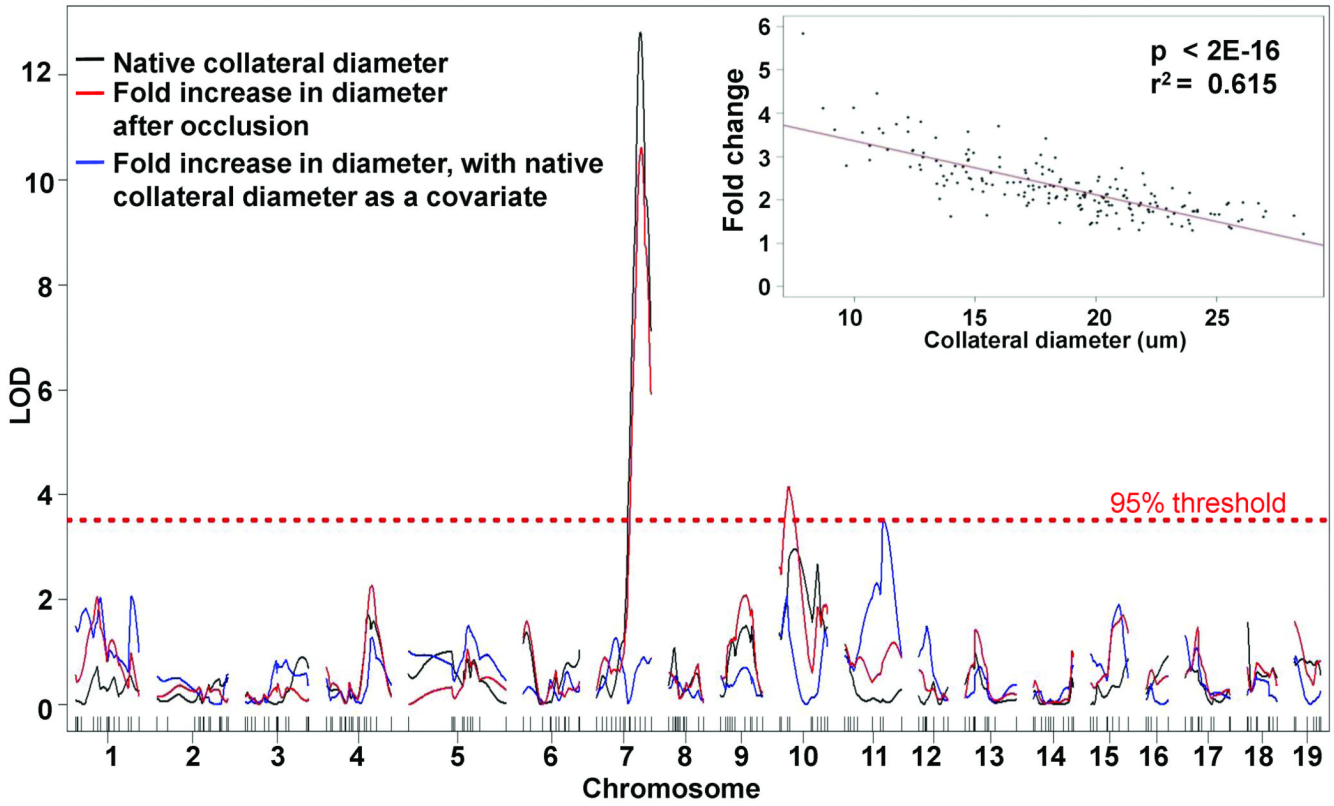

Figure 6. Collateral remodeling after MCA occlusion: Genome-wide mapping identifies a QTL on chromosome 11

Diameter measurements made in 190 F2 mice 6 days after right-side MCA occlusion were subjected to single QTL mapping. Black curve, native collateral diameter (non-occluded side); the LOD score is lower than in Figure. 1 because there were fewer mice (See Supplemental Methods). Red curve, fold increase in collateral diameter after remodeling (occluded over non-occluded). Blue curve, fold increase in diameter after rescanning with native collateral diameter as a covariate (see inset for close correlation between fold increase in diameter in the right hemisphere and native collateral diameter). The chromosome 7 QTL for remodeling (red curve) was lost (blue curve), but a QTL for remodeling on chromosome 11 achieved significance (*Carq1*, Table 1; $p<0.05$).

Table 1

Chromosome location, LOD score, confidence interval and genetic descriptors of collateral QTL identified using multiple QTL model.

Trait	QTL	Chr	Location *	LOD	95% CI †	Effect size ‡	Additive ± SE§	Dominance ± SE§	P value
Number	Canq2	1	45.0 (90)	12.6	38–49	13.3	−1.09 ± 0.22	0.34 ± 0.32	6.3E-10
	Canq3	3	5.0 (18)	6.6	0–28	6.3	0.09 ± 0.22	-0.15 ± 0.31	1.1E-04
	Canq1	7	63.6 (134)	28.7	62–65	37.2	−2.67 ± 0.22	1.42 ± 0.30	< 2.0E-16
	Canq4	8	16.8 (47)	5.0	6–24	4.9	0.85 ± 0.21	−0.67 ± 0.31	2.2E-05
	1:3			6.6		6.2			1.8E-05
Diameter	Cadq1	7	64.0 (134)	17.2	61–66	30.0	−3.25 ± 0.35	1.68 ± 0.49	1.8E-04
Conductance	Cacq2	1	47.3 (106)	6.0	31–81	6.6	−27.27 ± 5.05	0.18 ± 7.07	1.1E-06
	Cacq1	7	64.0 (134)	30.5	62–66	44.0	−67.90 ± 5.06	28.31 ± 7.07	< 2.0E-16
Remodeling	Carq1	11	55.6 (93)	3.5	41–72	8.1	0.15 ± 0.01	−0.03 ± 0.01	<0.05

*Location; cM (Mb);

†Confidence interval, cM;

‡Percent of the total phenotypic variation explained by locus.

§Additive or dominance coefficients;

SE, standard error of the mean.

Table 2

Candidate genes resulting from EMMA analysis of chromosome 7 QTL locus.

Start (bp)	Symbol	Orient	E	Description
132362957	LOC670828	−	protein	similar to 40S ribosomal protein S7 (S8)
132476076	4933440M02Rik	−	mRNA	RIKEN cDNA 4933440M02 gene
132554205	LOC100043014	−	protein	predicted gene 4171
132588190	Jmjd5	+	best RefSeq	jumonji domain containing 5
132611162	Nsmce1	−	best RefSeq	non-SMC element 1 homolog (S. cerevisiae)
132690783	EG244214	+	mRNA	predicted gene, EG244214
132695796	Il4ra	+	best RefSeq	interleukin 4 receptor, alpha
132746991	Il21r	+	mRNA	interleukin 21 receptor
132784468	Gtf3c1	−	best RefSeq	general transcription factor III C 1

Genes in grey area have $p < 2.2 \times 10^{-5}$ genes in white area have $p < 4.17 \times 10^{-4}$. Orient, orientation of transcription.